Modern Instrumentation, Application, and Analysis of Brownian Motion

Blake Cole

*This work was submitted as part of a course requirement for completion of the BS degree in the Physics Program at RIT and, in its current form, does not appear in any publication external to RIT.**

(Dated: April 28, 2020)

The effectiveness of studying Brownian Motion has improved significantly since the advent of digital recording devices. In the past, this experiment was conducted by viewing suspended particles through a microscope and attempting to track the particles by marking paper at regular intervals. Utilizing a high frame rate digital camera and specialized particle tracking software improves the efficacy of this experiment significantly. So much so, that this method can now be used to study the visco-elastic properties of the solution. During Capstone 1, this project designed an experimental procedure, and collected data from samples of pure water containing microbeads. In Capstone 2, the accuracy of the data was analyzed and the viscosity of solutions containing various ratios of glycerol was studied. These experiments found that the procedure described in this paper produced viscosity data that were consistently within two standard deviations of theoretical values.

Background

Brownian Motion was first observed by Robert Brown when he saw chaotic motion of tiny pollen particles suspended in water, originally he thought this might be due to biological organisms. Albert Einstein later theorized that this motion resulted entirely from the atomic nature of matter and could be explained as collisions between the particle and the molecules of the solution.[1] Einstein's hypothesis was tested by the French physicist, Jean Baptiste Perrin, who had developed a technique for creating precise spherical particles around 1×10^{-6} meters (1μm) in size. To observe the chaotic motion, the particles were suspended in water and observed through a microscope and camera lucida, which allowed the image of the microscope slide to be superimposed on a drawing surface. The position of the particles were then marked at regular time intervals.[2] This experimental process can be greatly improved by using a digital camera and particle tracking software.[3]

Theory

The motion of the suspended particle can be modeled as the sum of the impulses on the particle during a given instance (dt). Consider the interaction between one molecule of the solution and the particle being studied. During the collision the particle is subject to a force $F_i(t)$. Over a given time dt the impulse of this force is defined as:

$$J_i = \int F_i(t)dt \tag{1}$$

Given the relative size difference between the particle and the individual molecules which comprise the solution, one can imagine many thousands of impulses in a short time dt. The total force on the particle during a given time dt is the sum of all such impulses.

$$F(t)dt = \sum_i J \tag{2}$$

Where $F(t)$ is given by Paul Langevin's equation describing a viscous fluid:

$$F(t)dt = -\alpha v(t)dt + F^{(r)}(t)dt \tag{3}$$

and where α is the viscous drag coefficient. Studied by Stokes and found to be

$$\alpha = 3\pi\eta d \tag{4}$$

for sphere of diameter d in a fluid with viscosity given by η. That term causes the particle's velocity to tend towards zero, while $F^r(t)$ represents the random force applied by thousands of particulate collisions, causing it to accelerate once again, and giving rise to the particle's chaotic motion. The randomly applied force $F(t)$ creates a distribution in the particle's velocity. Specifically, one that satisfies the equipartition theorem, which states that the kinetic energy of the molecules in a system is proportional to the temperature.[4] In one dimension this can be expressed as:

$$\frac{1}{2}m\langle v_x^2\rangle = \frac{1}{2}K_B T \tag{5}$$

where m is the mass, T is the temperature, K_B is the Boltzmann constant, and $\langle v_x^2\rangle$ is the average velocity for a large population size. The underlying statistics governing the chaotic motion come from an application of the central limit theorem, which states that if many numbers are randomly drawn from the same probability distribution, the sum of these numbers will be a Gaussian-distributed random number.[3]

Specifically the theorem predicts that N random numbers drawn from any probability distribution, with a mean of μ_i and variance σ_i^2, then the sum of those numbers $\sum N$ will result in a Gaussian distribution with mean $\mu = N\mu_i$ and a variance of $\sigma^2 = N\sigma_i^2$.

In the study of Brownian Motion the mean displacement (Δr) of the particle is equal to zero, since the displacement in either direction is equally likely. However the mean squared displacement (MSD) is the variance of the resulting Gaussian.[4] In one dimension:

$$\sigma^2 = \langle \Delta r^2\rangle = \langle \Delta x^2\rangle = 2Dt \tag{6}$$

where D is the diffusion coefficient defined as:[5]

$$D = \frac{K_B T}{\alpha} \tag{7}$$

Einstein was the first to theorize a correlation between the Diffusion Coefficient (D) and the variance of the distribution. This created an important link between viscosity, temperature of the solution, and the random motion exhibited by a suspended particle.[3] Einstein's theoretical description forms the basis for this study of Brownian Motion.

Experimental Design

These theoretical predictions can be studied by using a digital camera with a fast frame rate in combination with a microscope. This can be achieved by using a trinocular microscope design, which allows a camera to be easily attached and shares an optical path with the traditional eyepieces. For this experiment, a traditional binocular microscope was modified by removing one of the eyepiece lenses and a digital camera was mounted using set screws. The camera used for this was a DMK 33UX178 purchased from Imaging Source, with a frame rate up to 60 frames per second. Using the propriety software that comes with the camera, high frame rate footage was recorded of the sample on the microscope slide. The camera software allows gain and exposure to be adjusted until particles are most visible and contrast is high. A high contrast allows for easier particle identification later on.

The microscope slides were prepared in a way to reduce outside interference like wind currents. This was done by drawing a square with petroleum jelly on one slide, injecting the solution in the square shape, then placing another glass slide on top to create a seal. The solutions contained polystyrene micro particles, with a factory stated radius of 0.495 μm. The particles were donated from Dr. Thurston's lab at RIT and came in a solution of water and microparticles. 10 μl of this particle containing water was mixed with glycerol and more water in various ratios until the total liquid amounted to 100 μl. The solutions were combined by hand using a pipette until thoroughly mixed and uniform throughout. 20 μl of the sample solution was injected onto microscope slides using the previously described technique. The samples were allowed to settle for 10 minutes after being created in order reduce extraneous movements introduced during the injection process.

Random error can be reduced by using a larger sample size, so videos were recorded with several hundred frames at 60 fps, approximately 15 seconds. These videos comprised the data sets used in the study. In order to evaluate the accuracy of the experimental procedure, several samples slides were created of each ratio, then several videos were taken of each sample slide. The raw video data contained visible smudges, likely from the microscope lenses. To improve the accuracy of the particle tracking, the stationary background of the video was subtracting using the imaging software ImageJ.[6] The processed video was then split into individual frames and fed into a particle tracking algorithm. The algorithm was written in Python and utilized functions from a preexisting particle tracking library, TrackPy, based on work done by Eric Weeks. Complete documentation can be found at http://soft-matter.github.io/trackpy.[7] The before and after of background subtraction done with ImageJ is shown below.

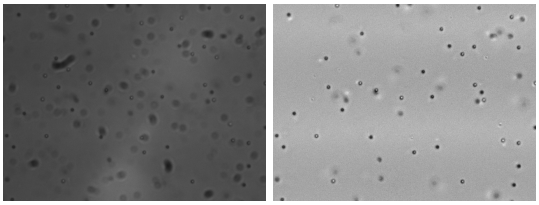

(a) before (b) after

FIG. 1: The video is processed with ImageJ using a background subtraction macro

After the video file is processed, the next step is to run the particle tracking software. There are important input parameters that may have to be adjusted for each trial, such as number of image frames, and most importantly particle brightness. A technique which proved helpful during this process was to initially analyze one frame with a brightness set to a low value. This allowed all the particles to be identified as well as some extraneous features. This step of particle identification is visualized by annotating the frame with red circles around the identified features.

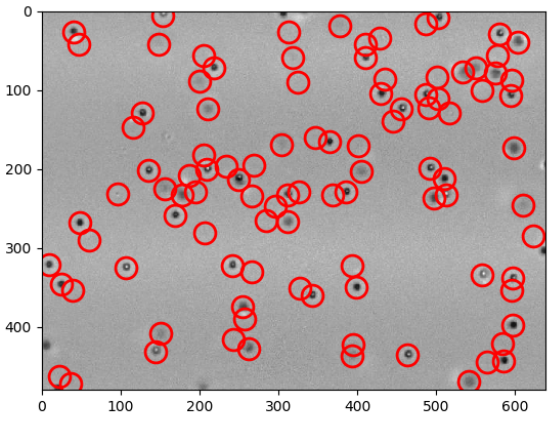

FIG. 2: The initial identification step which has intentionally identified extraneous features. This ensures each particle is tracked, then the extraneous features are filtered out in a later step.

Then a histogram is made after the first annotation/identification step, comparing number of features

identified with brightness (also referred to as mass).

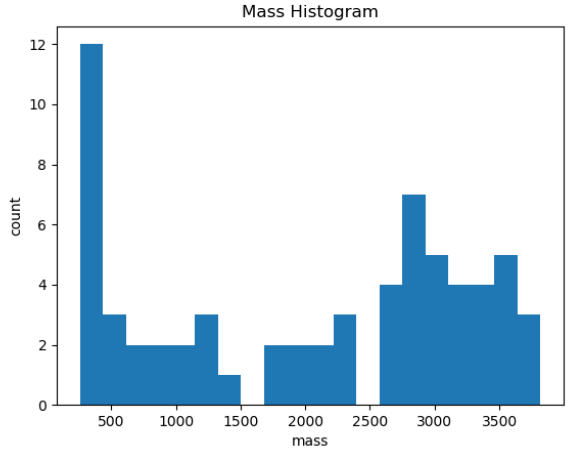

FIG. 3: A histogram comparing number of particles to the particle brightness (mass). This helps the user determine what to input for brightness (mass) in the following steps.

After viewing the histogram plot, the script waits for the user to input a value for particle brightness. The frame is then redrawn with annotated features based on the supplied value. This technique allows us to first get an estimation for brightness based on the histogram, then verify that the algorithm is identifying particles accurately. Once the user has verified particles are being cor-

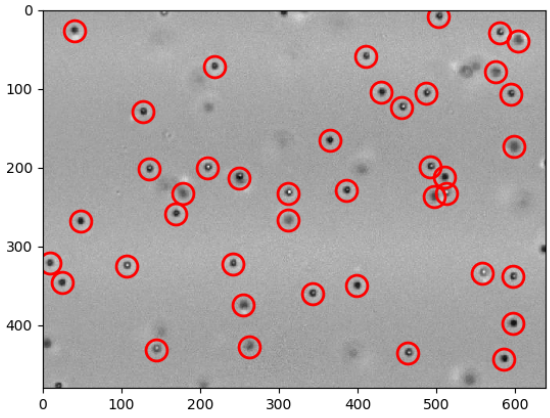

FIG. 4: Based on user input, only particles in focus are now identified for tracking.

rectly identified, a batch analysis is run on all frames in the video. With the parameters set, the script analyzes each frame of the video, calculates individual particle displacements, and then links the displacements throughout all frames to create a trajectory for each particle. Shown in Figure 5 is an example of one such trajectory plot.

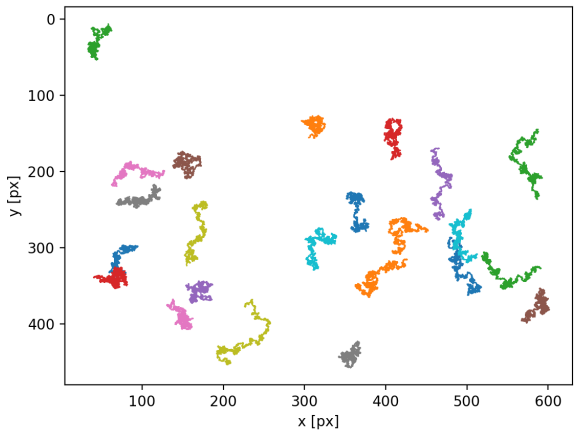

FIG. 5: Trajectory plot for many particles over the course of several hundred frames.

Creating these trajectories is dependent on the algorithm identifying and tracking each particle separately. This involves parameters such as the max displacement a particle can have between frames, and how many frames a particle must be present for in order to be counted. A high frame rate camera allows for more accurate tracking, since the particle displacement between frames can be set very low (1-2 pixels). In addition, it was found that setting the number of frames for which the particle is visible, to a high percentage (95%) of the total video frames ensured that only consistently visible particles were tracked, which improves accuracy in subsequent calculations.

The Trackpy library includes a drift-subtraction routine which greatly helps accuracy by removing the overall drift, which is often present in the samples despite efforts to isolate the system. After removing the drift and vibrational noise, the Mean Squared Displacement (MSD) and averaged or Ensemble Mean Squared Displacement (EMSD) can be calculated and plotted.

This plot can give great insights into the fluid properties of the solution. For particles undergoing stochastic processes we expect this to be a linear trend, essentially displacement is linearly correlated with a time interval. Hypothetically if the solution was undergoing an active process, such as ion transport, we could expect an overall positive slope indicating directed motion. One can imagine several scenarios that might be reflected in the MSD plot and these could be the study of further experiments using this technique. From this data, a line is fit to the EMSD, slope is extracted, and the diffusion coefficient from the variance. A number of interesting values can then be calculated using the diffusion coefficient including; the Bolzmann constant, Avagrado's number, the radius of the bead, the ideal gas constant, and the temperature of the solution.[5] These would be typical calcu-

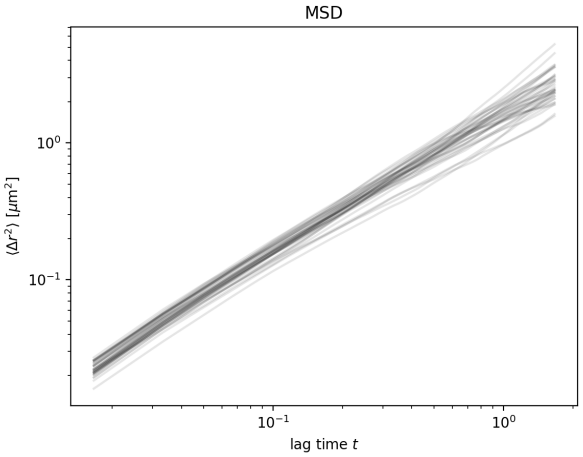

FIG. 6: Plot of Mean Squared Displacement for individual particles over the course of several hundred image frames.

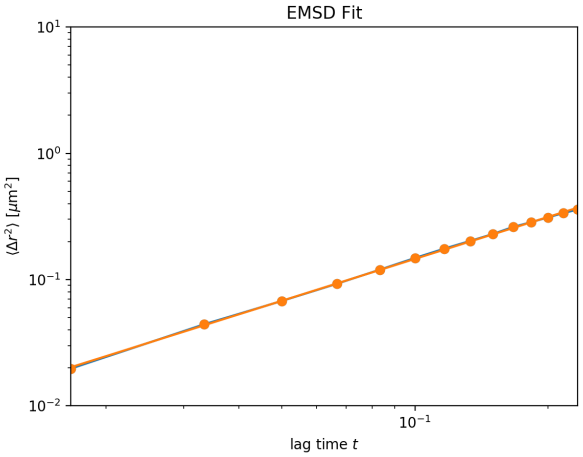

FIG. 7: An average of the individual MSD's from the previous figure, plotted with a fit line. This EMSD data is used to calculate the diffusion coefficient.

lations performed in an undergraduate laboratory. The results produced in this project are described in the next section.

Data Collection and Analysis

During Capstone 1 the experimental procedure was done with solutions containing microbeads and pure water. During Capstone 2, the procedure was performed with solutions of various viscosities. These were solutions of microbeads, water, and various amounts of glycerol. The samples analyzed were prepared in ratios 0%, 20%, 40%, and 50% glycerol to water. For the sample of pure water, the diffusion coefficient was found by averaging the results from 5 separate samples and 40 different trials total. The diffusion coefficient was found to be $0.45 \pm 0.02 \mu m^2/s$, within one sigma of the nominal value $0.445 \mu m^2/s$, found by Catopovic et al..[5]

The diffusion coefficient was then used to calculate the Boltzmann constant and compared with the known value. Those values are compared in table I.

Theoretical	$1.38 \times 10^{-23} J/K$
Measured	$1.26 \pm 0.05 \times 10^{-23} J/K$

TABLE I: Value of Boltzmann Constant calculated using our value for the Diffusion Coefficient versus the accepted value. Our value agrees within 3 sigma.

For the viscous solutions of glycerol and water, the diffusion coefficient was used to calculate the dynamic viscosity of the solution. There is no theoretical model for the viscosity of an arbitrary mixture of two fluids. Thus we have used models developed specifically for solutions of glycerol and water. The theoretical values were obtained from models created by Andreas Volk and Christian Kähler[8] based on modifications to work done by Nian-Sheng Cheng[9]. The scope of data collection was limited due to the ongoing COVID-19 pandemic, however for mixtures of 20% and 40% a minimum of 3 samples and 30 trials were taken. For the 50% mixture 1 sample was studied in 8 trials, thus the data is considered insufficient but included for completeness. The results of these trials are summarized in table II.

Percent Glycerol	Measured Viscosity	Theoretical Viscosity
20%	1.9±0.1 mNs/m^2	1.77 mNs/m^2
40%	4.0±0.2 mNs/m^2	4.18 mNs/m^2
50%	6.31±0.02 mNs/m^2	7.12 mNs/m^2

TABLE II: Viscosity values for 40% and 20% agree within 1 and 2 sigma respectively. The data collected for 50% is considered insufficient. Sources of error for these values is discussed in the following section

The results of these trials were averaged, including the sample of pure water, and plotted against a curve of theoretical viscosity values for a temperature of $24°C$.

In addition, the measured values were plotted against theoretical values and fit with a line. For a perfectly accurate experiment the slope of this line would be equal to 1. The resulting slope had a value of 1.10 with a percent error of 0.03. A value 10% higher than perfect accuracy. This suggests that there could be a systematic error causing the measured values to be consistently lower than theoretical. The potential source of this error is discussed in the next section.

The ultimate goals of this capstone project were to collect more samples at different viscosities in order to

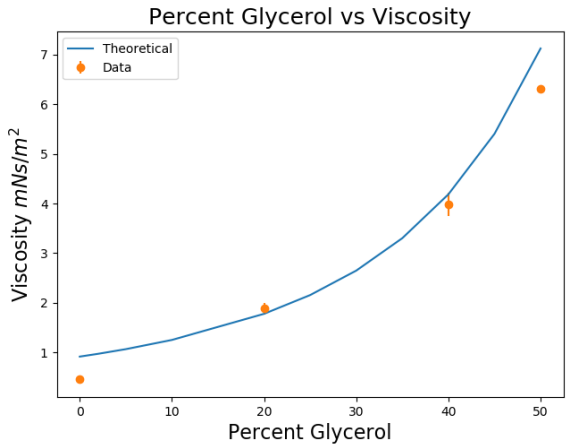

FIG. 8: The data falls both above and below the curve of theoretical values suggesting there is not a significant source of systematic error. With more data collection the error could be better estimated.

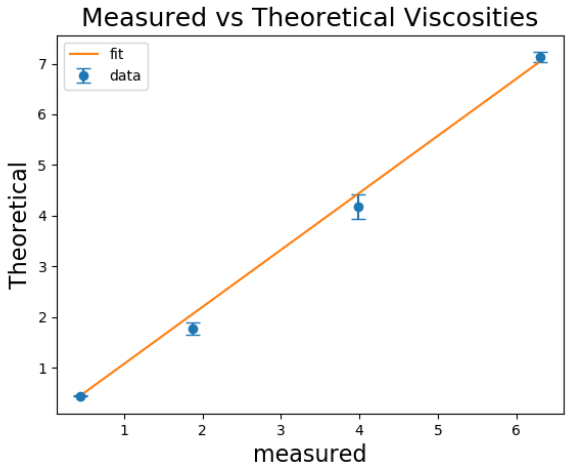

FIG. 9: Measured values that perfectly match theoretical would have resulted in a slope of 1. The resulting slope was m=1.10 ±0.03.

more accurately gauge the effectiveness of this experimental technique, then continue experimentation with visco-elastic solutions. These solutions would have had different properties and result in different particle motion behaviour which could have potentially been analyzed using the Mean Squared Displacement data in a similar way. However the data obtained thus far shows that the measured values are within 10% of the theoretical calculations, making this a viable experiment for an undergraduate scenario.

Sources of Error

The level of accuracy obtained was the result of improving the experimental technique throughout Capstone 1 and 2. For example, visible spherical aberrations were reduced by restructuring the camera mounting system, which allowed the particles to be more accurately viewed through the lenses, and thus more accurately tracked. Preparation of the microscope slide was also improved simply by repetition. Besides improvements to the physical set up, the software implementation was also improved. By repeating trials with slight variations and comparing results, the key input parameters for accurate particle tracking become more obvious. For example, accurately choosing the max displacement between frames saw almost a 20% difference in values, whereas setting the diameter as a tuple saw virtually no change in the calculated values.

Another important parameter is the particle lifetime, or the number of frames it is visible for. Setting this to a high percentage of the total frames means that only particles which are consistently visible will be tracked. Knowing which parameters can remain the same throughout trails and which parameters need to be tuned for the specific trial allows the experiment to be carried out with more efficacy. Despite these improvements work can still be done to increase the accuracy. It has been shown theoretically that the error in this method is primarily due to sampling error, measurement uncertainty (temperature, radius), tracking error, and vibrational noise and drift.[5] The method used in this paper attempts to correct for overall particle drift, so theoretically the error is produced by sampling error, tracking error, and uncertainty in measureables like temperature and particle radius.

As shown in the table below, the temperature on or near the microscope slide increases with time. These measurements were done using a Black and Decker laser thermometer. The large temperature variations in time

Time	Temperature (F)
0 minutes	71
8 minutes	72
20 minutes	74
30 minutes	77

TABLE III: Temperatures measured on the microscope slide with a laser thermometer after the microscope light was left on for the stated time.

is likely due to the older design of the microscope and inefficiency of the halogen bulb, which creates a considerable amount of heat if left on for an extended period of time. In order to reduce uncertainty in temperature, the microscope lighting element was turned off when not in use and only left on when recording video data. By reducing excess heat from the light source (like that shown

in the table), we expected the temperature of the slide to be relatively close but slightly higher than the room temperature. The room temperature itself is subject to fluctuations, especially considering the time period for data collection was on the scale of months. Using room temperature data that was collected during previous experiments, and the time vs heat data, the temperature on the microscope slide was estimated to be 24°Celsius. This was likely the largest source of random error in our experimentation. As discussed in Catipovic's detailed analysis of error sources, a temperature uncertainty of 1°C would create a 2% uncertainty in the macroscopic viscosity.[5] This estimate seems reasonable for our experimental set up. Using the measured value for diffusion coefficient in pure water, we calculated the Boltzmann constant to be $1.26 \pm 0.05 \times 10^{-23}$ J/K. Compared to the nominal value of 1.38×10^{-23} J/K. Assuming our value of diffusion is correct, the temperature would be equal to 21.8°C in order to accurately calculate the Boltzmann constant, as discussed this would also change value of viscosity. This loose calculation gives us an estimate of the uncertainty in temperature which falls slightly outside the 2% range previously described. Measuring the temperature across a microscope slide is a known issue for temperature dependent microscopy experiments.

Another source of random error is fluctuations in the particle diameter. The beads used in this experiment are stated to have an accuracy of 0.01 μm. Utilizing Trackpy's built in drift-subtraction routine should correct for systematic errors in drift. Since Brownian Motion is a stochastic process, it follows Poisson statistics, and taking more samples should reduce the error, which is why each data set consisted of several hundred image frames.

Conclusion

The experimental procedure developed during this Capstone project produced results that were within an accuracy range acceptable for the Modern Physics Laboratory. The procedure could be documented and turned into a laboratory experiment for the Modern Physics course. During Capstone 2 we demonstrated that this technique can be used to evaluate the viscous properties for different solutions. The experimental work was interrupted by the ongoing COVID-19 pandemic. Given more time we would have tested the limits of viscosity analysis by using higher concentrations of glycerol and potentially pure glycerol or other viscous solutions. In addition the rheological properties of visco-elastic solutions could have been analyzed through a process known as microrheology. This is considered a novel way of performing rheology, as typical experiments involve a relatively expensive piece of equipment called a rheometer and large amounts of solutions. This project has help to show the validity of doing these types of experiments using relatively inexpensive equipment and set up.

Acknowledgments

Special thanks to Dr. McLane, Dr. Bhattacharya and the Capstone Committee, the Gosnell School of Life Sciences for donating the microscope, Dr. George Thurston for donating the microspheres, and James Tillapaugh for creating the camera adapter for the microscope.

* Rochester Institute of Technology, School of Physics and Astronomy, Faculty Advisor: Dr. Louis McLane

[1] A. Einstein, *Investigations on the Theory of The Brownian Movement* (Dover, 1926).
[2] L. Brubacher, *An experiment to measure Avogadro's constant. Repeating Jean Perrin's confirmation of Einstein's Brownian motion equation*, CHEM 13 NEWS **1**, 14 (2006).
[3] R. DeSerio and S. Hagen, *Brownian Motion*, Macromolecules **29**, 1 (2015).
[4] K. V. D. Bogart, *Brownian Motion*, University Chicago Department of Physics Wiki (2019).
[5] M. A. Catopovic, P. M. Tyler, J. G. Trapani, and A. R. Carter, *Improving the quantification of Brownian Motion*, American Journal of Physics **81**, 485 (2013).
[6] W. S. R. . K. W. E. Caroline A Schneider, Nih image to imagej: 25 years of image analysis.
[7] D. Allan *et al.*, soft-matter/trackpy: Trackpy v0.4.2, 2019.
[8] A. Volk and C. J. Kähler, *Density model for aqueous glycerol solutions*, Experiments in Fluids **59** (2018).
[9] N.-S. Cheng, *Formula for the viscosity of a glycerol-water mixture*, Industrial & Engineering Chemistry Research **47**, 3285 (2008).